Research on Chemical Intermediates
https://doi.org/10.1007/s11164-024-05279-5

KF/MgO used as the catalyst for transesterification of dimethyl carbonate with isosorbide to dicarboxymethyl isosorbide

Xiafeng Yang[1,2] · Xin Long[1] · Jianguo Li[1] · Qingyin Wang[1] · Gongying Wang[1,2] · Guangyuan Zhou[2,3]

Received: 15 January 2024 / Accepted: 23 March 2024

Abstract
Solid alkali KF/MgO catalysts were prepared using the impregnation method by combining alkali metal compounds with oxides, which performed the transesterification of isosorbide (IS) with dimethyl carbonate (DMC) into dicarboxymethyl isosorbide (DC). Characterization of the catalysts was conducted through X-ray diffraction, scanning electron microscopy, Fourier transform infrared spectroscopy, and N_2 adsorption–desorption analysis. The catalytic performance of KF/MgO was examined under diverse KF loading and calcination temperature conditions. The characterization of catalyst identified that the creation of innovative active components K_2MgF_4 and K_2CO_3 were produced at a calcination temperature of 500 ℃ and a KF loading amount of 40%. The catalyst of 40-KF/MgO-500 demonstrated the most effective, favourable activity and selectivity. Through the optimization of transesterification process conditions, it was discovered that the yield of DC was at its highest under the optimal reaction conditions of n(DMC)/n(IS) = 6.5, catalyst dosage of 0.21 wt% (relative to IS mass), transesterification temperature of 120 °C, and reaction time of 6 h.

Keywords Transesterification · Solid base catalysts · Isosorbide · Dimethyl carbonate

Introduction

The employment of petroleum-based polymer materials has led to the gradual depletion of petroleum resources and environmental pollution [1, 2]. Consequently, the quest of polymer material's researchers is to utilize renewable resources. Nevertheless, isosorbide (IS), which is a bio-based renewable resource [3], can be promptly transformed from glucose and cellulose [4–6]. The implementation of isosorbide-based chemicals and materials has garnered significant interest from domestic and

Extended author information available on the last page of the article

Published online: 26 May 2024

international researchers. Through extensive research, it has been demonstrated that IS, characterized by its unique, inflexible structure, is considered to be the most promising candidate to substitute bisphenol A in polycarbonate production [7–9]. Particularly, isosorbide and its derivatives present compelling monomeric agents for bio-based polymer synthesis, comprising polycarbonates [10, 11], polyesters [12], polyamides [13], and polyurethanes [14], as they exhibit exceptional performance and optimal compatibility [15, 16].

Isosorbide-based polycarbonate (IS-PC) is a material with non-toxic properties and excellent optical, scratch-resistant, and thermal stability. It is also biodegradable, biocompatible, and has great potential for applications in packaging, automotive, electronics, electrical appliances, and biomedicine [17]. IS-PC is mainly prepared by melt transesterification, which is primarily accomplished through the reaction between an ester and one or more alcohols, acids, or esters at elevated temperatures [18]. This preparation method has the advantages of simple process, green environmental protection, easy availability of raw materials, no toxic solvents, and high product yield, which has become the development direction of IS-PC preparation technology. Currently, IS and either diphenyl carbonate (DPC) or dimethyl carbonate (DMC) is commonly used as raw materials in the preparation of IS-PC [19], as displayed in Formula (1). This approach enables the recycling of phenol or methanol as by-products, which can then be repurposed to produce DPC or DMC [20]. Although IS-PC produced via the DPC method exhibits high molecular weight and performs relatively well, DPC is synthesized using DMC [21], which involves a lengthy process and fetches a significantly higher market price than DMC. During the reaction process, a significant amount of high boiling point by-product phenol is produced, which can impact material properties and hazard to human health [22]. The usage of DMC as raw material for preparing IS-PC has several advantages, including a shorter process, lower production costs, and better environmental performance [23, 24]. As catalytic technology and processes continues to advance, this method is expected to become the leading and most competitive route for preparing IS-PC.

Currently, the development of IS-PC via the DMC technique presents certain challenges and is still at the laboratory research stage. When considering raw materials, DMC has a low boiling point that makes internal temperature control difficult due to its vaporization under heat. And about IS has a tendency to deliquesce and possess a significant steric hindrance. Moreover, the internal hydroxyl group within

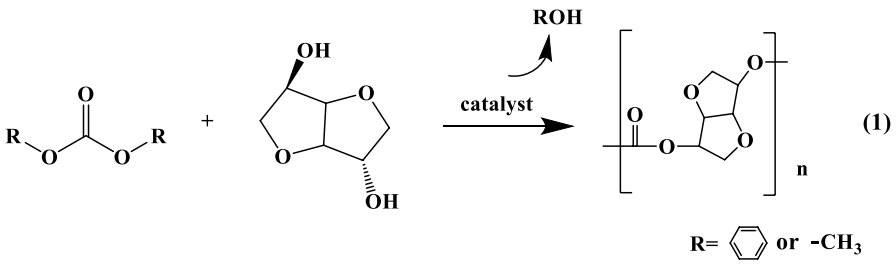

Formula 1 Reaction formula for preparing IS-PC

its molecular structure can form an intramolecular hydrogen bond with the oxygen in another furan ring, which causes a large difference between internal and external hydroxyl activity. Consequently, this results in a low efficiency reaction [25–27]. From the point of view of reaction, the strong electrophilicity of carbonyl carbon and methyl carbon in DMC result in carboxymethylation and methylation side reactions in the course of the transesterification reaction stage [28]. Refer to Fig. 1 for a visualization of the reaction.

As shown in Fig. 1, the DMC method-prepared IS-PC transesterification reaction may result in eight products. Among them, the intermediate product dicarboxymethyl isosorbide (DC) obtained from monocarboxymethyl isosorbide resolves the issues of hydrophilicity and low reactivity of IS due to its molecular structure containing -$OCOOCH_3$ group, which provides a prerequisite for the synthesis of IS-PC with high molecular weight and high performance [29–31]. Additionally, DC can

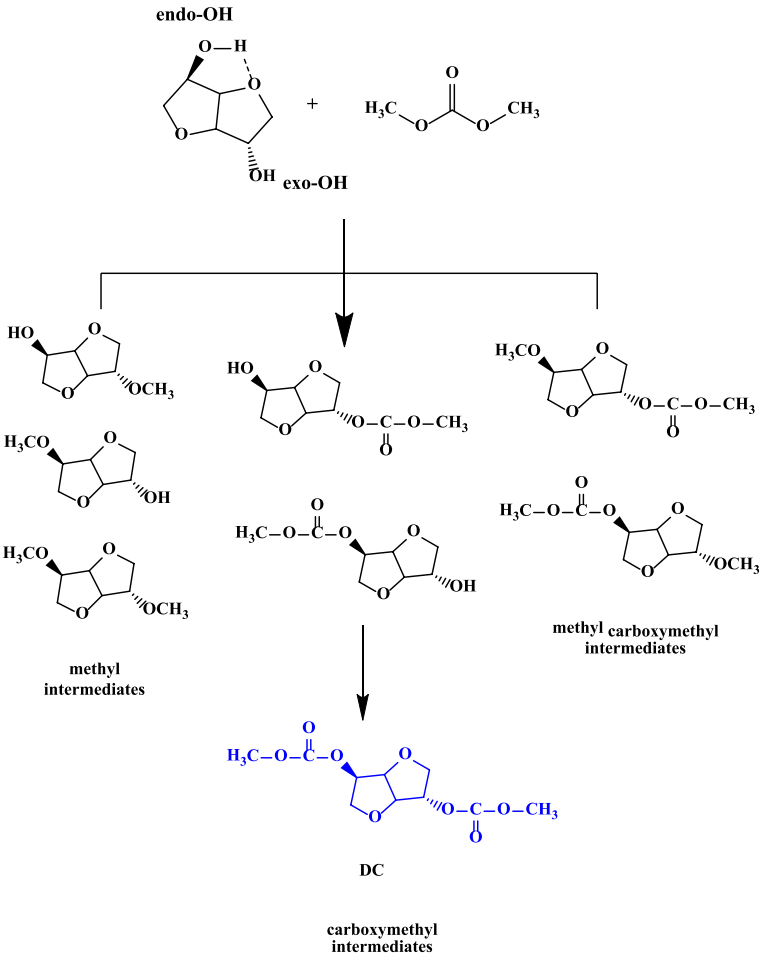

Fig. 1 Process of the transesterification reaction between DMC and IS

act as a plasticizer, decreasing the material's melting temperature and melting viscosity. This improves the material's processing performance, flexibility, and optical transmittance.

At present, researchers still commonly use the traditional one-pot method by using controlled ionic liquids or traditional solid bases as catalysts to synthesize IS-PC. However, the exploration of its ester exchange phase has been rarely reported, and conformational relationships between reaction processes and catalysts has not been comprehensively studied. In addition, ionic liquid as a homogeneous catalyst, the retention of its anions and cations may cause yellowing of the material and a decrease in the relative molecular mass, limiting the use of IS-PC in many fields, particularly those with high standards for product transparency and aesthetics. About traditional solid bases merely a minor number of catalysts exhibit favourable selectivity for DC synthesis [23], including caesium carbonate (Cs_2CO_3), lithium acetylacetonate (LiAcac), and potassium carbonate (K_2CO_3). However, separating these alkali metal salts poses difficulty, leading to metal ion residue which adversely affects subsequent IS-PC [26].

In this paper, solid base KF/MgO catalysts with simple separation, remarkable activity, and exceptional stability were created through the impregnation method for transesterification aimed at synthesizing DC. The study systematically explored the impact of catalytic performance on the DC yield during transesterification. The study investigated the structure–activity relationship of KF/MgO during the reaction using X-ray diffraction (XRD), scanning electron microscopy (SEM), N_2-adsorption–desorption, alkalinity, and base quantity analysis, and Fourier transform infrared spectroscopy (FT-IR). Furthermore, the transesterification reaction conditions of isosorbide and dimethyl carbonate were optimized. Finally, a high-yield DC was synthesized, providing a foundation for producing high molecular weight and high-performance IS-PC.

Experimental

Materials

Dimethyl carbonate ($C_3H6O_3, > 98\%$), acetone ($C_3H_6O, > 98\%$), and methanol ($CH_3OH, > 98\%$) were purchased from Chengdu Ke-Long Chemicals Reagent Co., Ltd. (Chengdu, China). Isosorbide (IS, > 99%) was purchased from Jinan Yu-Ten Pharmaceutical Co., Ltd. (Jinan, China). Potassium fluoride (KF, > 98%) was purchased from Shanghai Adamas Reagents Co., Ltd. (Shanghai, China). Nano magnesium oxide (MgO, > 98%) was purchased from Shanghai Diper Biotechnology Co., Ltd. (Shanghai, China).The deionized water used in the experiment was made homemade by the laboratory.

Preparation of catalysts

KF/MgO was prepared via a wet impregnation method. In standard preparation, an appropriate quantity of KF aqueous solution was added to MgO and stirred for 6 h. The resulting mixture was subjected to rotary evaporation to remove water.

The powder was then ground and calcined in a muffle furnace at a temperature of 300–700 ℃ for 5–8 h. The resulting material was designated as x-KF/MgO-T, where x and T represent mass fraction (%) and calcination temperature (℃), respectively.

Synthesis of DC

Under the protection of nitrogen purge, KF/MgO catalysts were added to a three-necked flask holding a thermometer and an air condenser tube, along with a specific raw material molar ratio. The transesterification reaction was conducted at a temperature range of 90–150 ℃. The reaction rate was enhanced by the continuous production of a DMC and MeOH azeotrope, as illustrated in Formula (2). After the reaction, the transesterification catalyst was filtered out and DMC was removed through vacuum distillation to obtain a high yield of the transesterification product dicarboxymethyl isosorbide.

Characterization of catalysts

X-ray diffraction (XRD) analysis was conducted on a Bruker D8 Advance diffractometer, utilizing Cu Kα1 radiation with a scanning speed of 5 °C/min within the 2θ range of 0.5° − 4.0°, at 40 kV and 100 mA. N_2 adsorption–desorption was measured using a Quantachrome Autosorb-IQ gas adsorption analyser. The BET equation was utilized to obtain the surface area. The BJH adsorption isotherm method was implemented to determine the pore size distribution of the catalyst samples. Fourier transform infrared spectroscopy (FT-IR) was conducted using Thermo Fisher Nicolet 670, and the catalyst underwent KBr methodology. The band range was 4000–500 cm^{-1} with a resolution of 4 cm^{-1} and temperature of 25 °C. Moreover, scanning electron microscopy (SEM) was employed to characterize the catalyst surface, utilizing ZEISS Gemini 300. The samples were adhered directly onto the conductive adhesive and subjected to 45 s of spraying and 10 mA using the Oxford Quorum SC7620 sputtering spreader. The voltage of acceleration used was 3 kV, and the detector employed was SE_2 for the secondary electron detection. The base strength (H_) and basicity of these samples was studied by employing the Hammett indicator alongside bromothymol blue (H_ = 7.2), phenolphthalein (H_ = 9.8), and 2,4-dinitroaniline (H_ = 15.0).

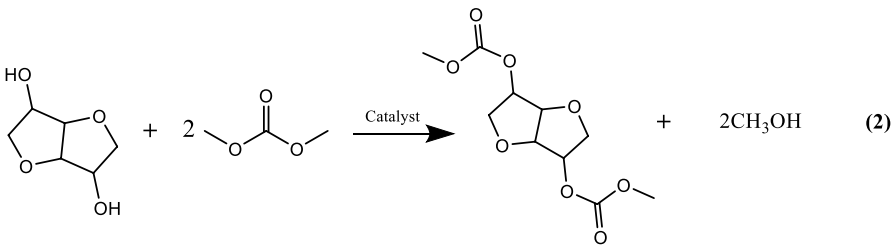

Formula 2 IS and DMC transesterification processes.

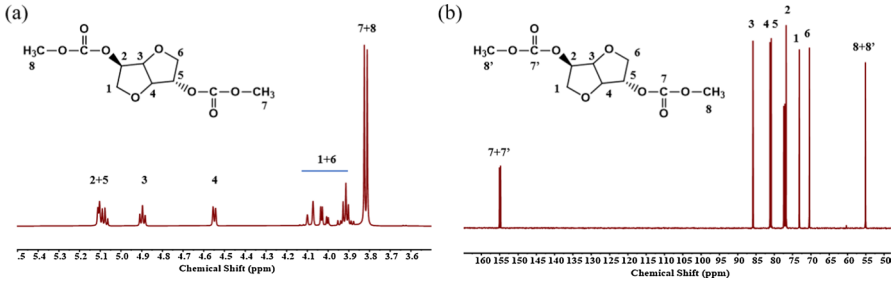

Fig. 2 Typical **a** ^{1}H NMR and **b** ^{13}C NMR spectra of DC prepared using KF/MgO

Results and discussion

The DC molecular structure was synthesized by melting transesterification reaction

DC as an important product of transesterification synthesis and also a prerequisite for the synthesis of IS-PC. The structure characteristics of the synthesized DC, catalyzed by KF/MgO, were determined by [1]H NMR and [13]CNMR spectra (Fig. 2). From the [1]H NMR spectra, the peaks of the ISB moiety unit at δ5.09–5.04, 4.87, 4.53, 4.08–4.00, and 3.93–3.85 ppm are assigned to hydrogen atoms recorded as 1, 2, 3, 4, 5, and 6, respectively. The terminal groups (–OCH_3) could be identified at δ3.80 and 3.78 ppm. As shown in [13]C NMR spectra, It similarly demonstrates the successful synthesis of DC using melt transesterification reaction.

Effect of catalyst preparation conditions on catalytic performance

KF/MgO has commonly been employed as a catalyst for transesterification processes, including the production of chemical intermediates and polyesters. However, its effectiveness in catalyzing the transesterification of IS with DMC for the synthesis of DC remains unexplored in the literature. The temperature at which the catalyst is calcinated and the amount of KF loaded onto the catalyst are crucial considerations in the course of the preparation process [32].

The 40-KF/MgO catalyst underwent calcination in the range of 0 °C-800 °C. Figure 3a illustrated the impact of varying calcination temperatures on the transesterification activity of the 40-KF/MgO catalyst. As observed in Fig. 3a, the uncalcined 40-KF/MgO demonstrated catalytic activity in effecting this reaction. While the conversion of IS was almost at 99.99%, the yield of MeOH and DC barely amounted to 80.3% and 47.5%, separately. The results demonstrated that the uncalcined catalyst exhibits higher activity, but lower selectivity. Interestingly, the conversion of IS and the yields of MeOH and DC were significantly lower when 40-KF/MgO was calcined at 200 °C compared to uncalcined 40-KF/MgO. It can be explained by the fact that the calcination temperature can alter the active centres of the catalysts. As the temperature for calcination increased, the number of original active sites decreased,

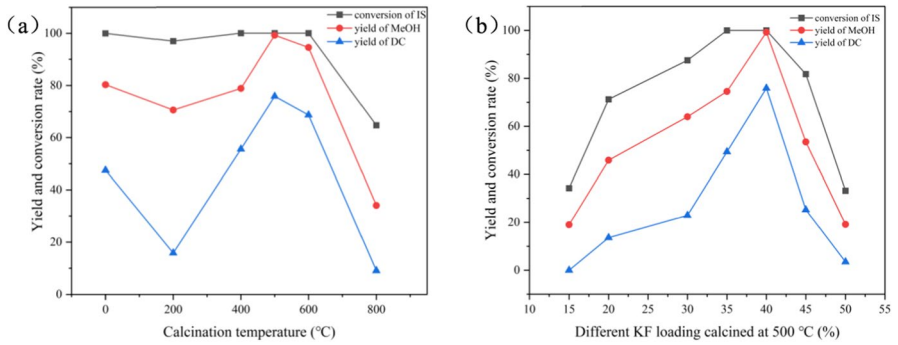

Fig. 3 **a** Effect of calcination temperature on the activity of 40-KF/MgO catalyst(40-KF/MgO dosage of 0.2 wt%, n(DMC)/n(IS) = 6.5, 8 h at 110 ℃ under ordinary pressure). **b** Effect of KF loading on the activity of KF/MgO-500 catalyst(KF/MgO-500 dosage of 0.2 wt%, n(DMC)/n(IS) = 6.5, 8 h at 110 ℃ under ordinary pressure)

and no new active sites were generated. This resulted in a significant decrease in the catalyst's reactivity, leading to a decrease in the reaction rate. When the calcination temperature of 40-KF/MgO increased from 200 °C to 500 °C, monocarboxymethyl isosorbide was gradually transformed into dicarboxymethyl isosorbide (DC), due to the yield of methanol was positively correlated with the yield of DC, While the yield of DC increased rapidly from 11.5% to 75.9%, and the yield of methanol increased from 70.6% to 99.2%. Then, it was found that high calcination temperatures of the precursor led to rapid decreases in the conversion of IS, as well as the yields of MeOH and DC. In conclusion, the active centre and pore structure of the catalysts were altered due to the higher calcination temperature, making them less active. Apparently, under the same reaction conditions, 40-KF/MgO-500 generated active centres and pore structures, which is the best facilitate melt-transesterification.

The KF/MgO-500 catalyst was loaded with a concentration of KF ranging from 15 to 50%. Figure 3b illustrates the impact of different loadings of KF/MgO-500 on IS converted to MeOH and DC yield. It can be inferred from Fig. 3b that the conversion of IS, MeOH and DC yield increased initially but subsequently decreased. The peak yields of MeOH and DC were attained at a KF loading amount of 40%, reaching 99.2% and 75.9%, respectively. However, the high loading of KF may have caused pore blockage in the catalyst, resulting in a rapid decrease in the yield of MeOH and DC. Therefore, 40-KF/MgO-500 displayed the highest catalytic activity during the reaction process and was selected for further investigation.

Optimization of reaction conditions

In order to determine the optimal conditions for the 40-KF/MgO-500 catalyst, a study was conducted on the impact of various reaction parameters on transesterification. Figure 4a displays the effect of reaction temperature on transesterification activity, demonstrating that the reaction of IS converted to monocarboxymethyl isosorbide and the production of DC occurred simultaneously between 90 ℃ and 110 ℃.

The conversion of IS increased significantly from 56.3 to 99.9%, while the yields of MeOH and DC rose rapidly from 31.4 to 99.1% and 5.1 to 75.9%, respectively. At a reaction temperature of 120 ℃, the conversion of IS remained relatively unchanged, whereas the yield of DC further increased, suggesting a faster rate of formation at this temperature. However, excessively high temperatures may have caused adverse reaction that produced methylated and other by-products, consequently reducing the yield of DC from 91.5 to 63.4%. The reaction process is displayed in Fig. 1. Therefore, 120 ℃ was identified as the optimal reaction temperature for further study.

Figure 4b displays how transesterification performance is influenced by the molar ratio of DMC and IS. As the n(DMC)/n(IS) ratio increased gradually from 1.6 to 3.3, the reaction of IS was nearly complete, but the yield of methanol was approximately 50%, and the yield of DC was not high. This consequence indicated that monocarboxymethyl isosorbide was mainly generated with the ratio of ingredients. The reaction process is depicted in Fig. 1. The molar ratio of DMC to IS affects the reaction rate of both processes. Further analysis indicated that the reaction rate of monocarboxymethyl isosorbide and dicarboxymethyl isosorbide formation was

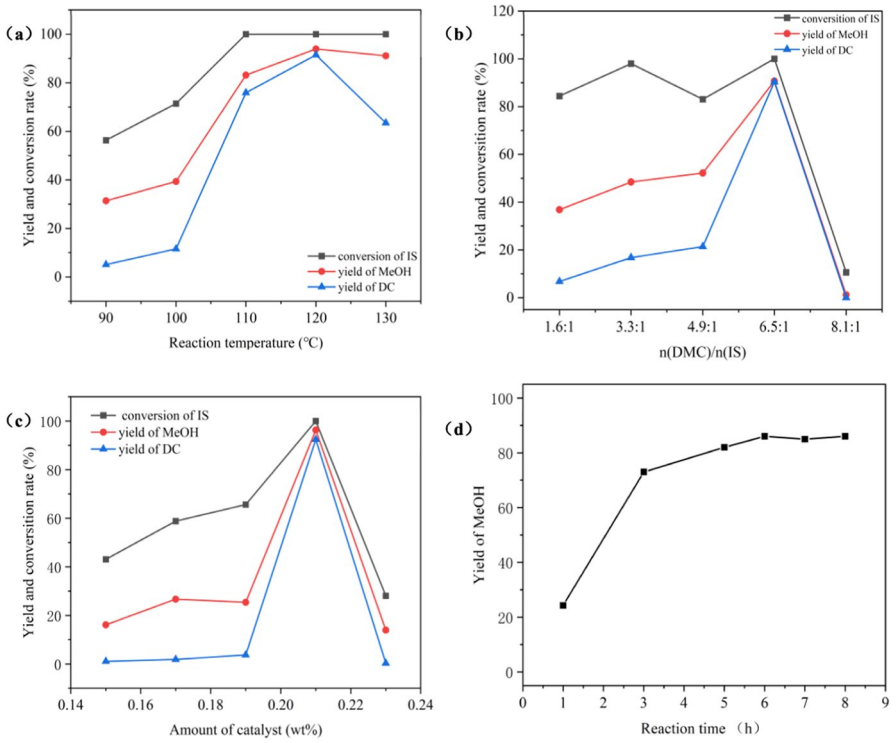

Fig. 4 **a** Effect of the reaction temperature (40-KF/MgO-500 dosage of 0.2 wt%, n(DMC)/n(IS) = 6.5 and reaction time at 8 h). **b** Effect of the n(DMC)/n(IS) (40-KF/MgO-500 dosage of 0.2 wt%, 8 h at 120 ℃). **c** Effect of Amount of catalyst (n(DMC)/n(IS) = 6.5, 8 h at 120 ℃). **d** Effect of reaction time (reaction temperature 120 ℃, n(DMC)/n(IS) = 6.5 and 40-KF/MgO-500 catalyst dosage 0.21 wt%)

impacted by the internal and external hydroxyl reactivity imbalance of IS when n(DMC)/n(IS) = 4.9. In this process, we speculate that the -$OCOOCH_3$ group within the structure of monocarboxymethyl isosorbide altered the distribution of its electron cloud and enhanced its hydroxyl activity. Consequently, the reaction rate for generating DC considerably exceeded that of converting IS to monocarboxymethyl isosorbide. This accounts for the decrease in the conversion of IS and the increase in the yield of methanol. When the ratio of n(DMC)/n(IS) = 6.5, the transesterification reaction was shifted to the right promoting equilibrium resulting in the highest selectivity of DC with a yield of 90.35%. However, it should be noted that DMC, which has a low boiling point, was heated and evaporated during the reaction. The excessive DMC that refluxed into the reaction system through the condenser lowered the internal temperature, always keeping it below 95 ℃. The reaction temperature failure led to a rapid drop in the conversion of isosorbide, the yield of methanol and DC. According to the results, the ideal raw material ratio was n(DMC)/n(IS) = 6.5, consistent with literature [24].

Catalysts are essential for producing DC during the transesterification stage [34], and their quantity has a direct impact on the yield of DC. The figure highlights that a small amount of catalyst is insufficient for transesterification. Figure 4c illustrates the impact of 40-KF/MgO-500 catalyst dosage on the transesterification reaction. When the catalyst amount was increased to 0.21 wt%, the active fractions in the reaction system increased, promoting the reaction to a certain extent and enhancing the conversion of isosorbide and the yield of MeOH and DC. Nevertheless, an excess of catalyst led to a concentration of free metal ions that was too high, resulting in side reactions and reduced yields of methanol and DC. Accordingly, the optimal catalyst amount of 0.21 wt% was selected for subsequent research.

Upon examination of the reaction equation, it is apparent that monocarboxymethyl isosorbide and dicarboxymethyl isosorbide were formed and contained MeOH. Therefore, the yield of MeOH can be used as an accurate indicator of the degree of reaction during the transesterification stage. The findings, depicted in Fig. 4d, demonstrated that the reaction was initially progressing rapidly in the early stages of transesterification. Among the hours of 3 and 5, the yield of MeOH increased at a sluggish pace, indicating a gradual decrease in the reaction rate as the reaction progressed. From 6 to 8 h, the rate of methanol collection remained relatively constant, suggesting that the transesterification reaction was complete. Consequently, 6 h represented the optimum reaction time.

Characterization of the catalysts

To obtain an understanding of the reaction mechanism for the transesterification of isosorbide and DMC catalyzed by KF/MgO, this study examined the interactions between KF/MgO and isosorbide or DMC through X-ray diffraction (XRD), scanning electron microscopy (SEM), Fourier transform infrared spectroscopy (FIRT), and N_2 adsorption–desorption.

X-ray diffraction

The XRD of KF/MgO catalysts with different calcination temperatures and KF loadings are shown in Fig. 5. The reason for the high efficiency of uncalcined KF/MgO in the transesterification reaction, but the low yield of DC, was investigated. Figure 5a illustrated that the presence of $Mg(OH)_2$, formed by the reaction between MgO and H_2O, promoted the transesterification reaction resulting in almost 99.99% conversion of IS. However, the presence of a small amount of crystals in 40-KF/MgO-0 resulted in the formation of strong hydrogen bonds between IS and the crystals. This increased the energy barrier of the hydroxyl group in IS to a certain extent and reduced the selectivity of the catalyst, resulting in a low DC yield. At a calcination temperature of 200 ℃, some of the $Mg(OH)_2$ decomposed into MgO, which leaded to a decrease in the catalyst's alkalinity and subsequently, a decrease in the rate of the transesterification reaction. This result is in agreement with the above statement. The variation of the calcination temperature from 200 to 500 ℃, the activated F^- induced in situ reaction of the oxide to form a new K_2MgF_4 diffraction peak (PDF 76–0038) (2θ = 13.4, 30.3 31.8 34.6 41.0 42.2 45.6 52.8 55.7 63.0). This led to easier activation of carbonyl groups in DMC and hydroxyl groups in isosorbide. The highest diffraction peak of K_2MgF_4 and the best catalytic activity are achieved at a calcination temperature of 500 ℃. This temperature effectively promotes the ester exchange reaction and results in the highest DC yield. On the other hand, if the calcination temperature is too high, the active centre K_2MgF_4 will disappear, and the pore structure will change, leading to a rapid decrease in the reaction rate and DC yield.

The X-ray diffraction (XRD) patterns of KF/MgO-500 catalysts with varied KF loadings are depicted in Fig. 5b. It has been verified that the characteristic diffraction peaks of MgO and K_2MgF_4 manifested at the calcination temperature of 500 ℃. As the KF loading increased, the intensity of the diffraction peak of K_2MgF_4 escalated gradually, leading to a rise in the number and intensity of active sites on the surface of the carrier and consequently promoting the reaction rate. The intensity of the K_2MgF_4 diffraction peak reached its peak at 40-KF/MgO-500, while the direct

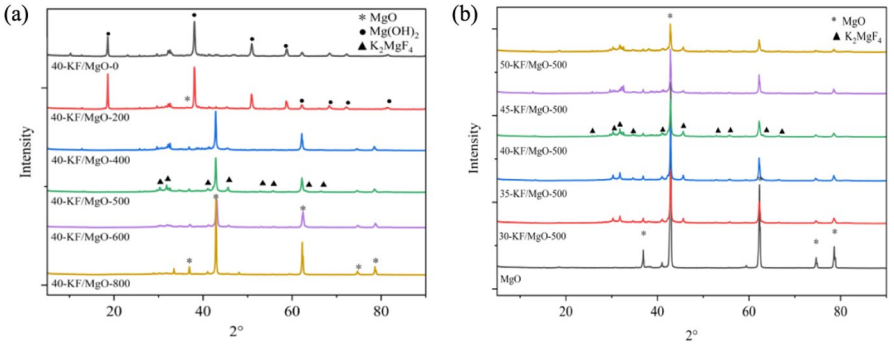

Fig. 5 **a** XRD patterns of 40-KF/MgO calcined at different temperatures **b** XRD patterns of KF/MgO-500 catalysts with different KF loadings

abortion rate was also at its highest due to the synergistic impact of alkaline strength and specific surface area. However, with KF loading above this threshold, the excess KF precipitated, obstructing the catalyst's pores and hindering the solid-phase reaction, which ultimately led to a decrease in the peak intensity, a reduction in reactive sites, and a rapid decline in the reaction rate. These findings align with the experimental process.

N_2 adsorption–desorption

In order to further clarify the structure–activity relationship of the catalyst in the transesterification reaction, the N_2 adsorption–desorption curves of KF/MgO catalysts with different KF loading and different calcination temperatures are shown in Fig. 6, and the parameters such as specific surface area and pore volume were summarized in Table 1. From Fig. 6, with the increase of gas pressure, it was apparent that multilayer adsorption occurs on the surface and pore wall of the porous material in the process of N_2 adsorption, capillary condensation occurs in the pore to form a typical H3 hysteresis loop, which belongs to the mesoporous structure. From Table 1, the specific surface area and pore volume of KF/MgO decreased with increasing KF loading. Typically, the higher calcination temperature causes the decomposition of the strong alkaline active centre K_2MgF_4, resulting in the collapse of the catalyst channel. The specific surface area of KF/MgO decreased from 6.29

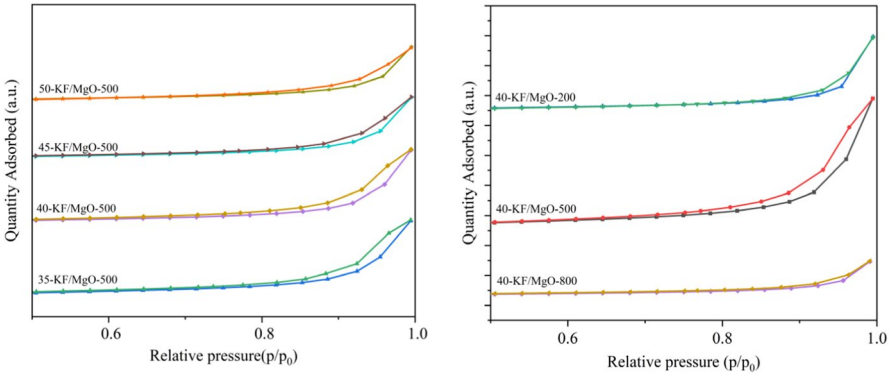

Fig. 6 N_2 adsorption–desorption isotherms of KF/MgO catalyst

Table 1 Specific surface area and pore volume of KF/MgO catalyst

Catalyst	S_{BET} (m^2/g)	Pore volume (cm^3/g)	Pore diameter (nm)
35-KF/MgO-500	7.12	0.038	19.97
40-KF/MgO-500	6.29	0.036	20.67
45-KF/MgO-500	5.10	0.031	15.66
50-KF/MgO-500	4.43	0.027	11.87
40-KF/MgO-200	2.95	0.020	15.33
40-KF/MgO-800	2.09	0.010	19.35

m [2]/g to 2.09 m [2]/g, the pore volume decreased rapidly from 0.036 cm [3]/g to 0.010 cm [3]/g.

Alkalinity and base quantity analysis

The basicity and base quantity of x-KF/MgO-500 and 40-KF/MgO-T were analysed by the Hammett indicator method. The results are summarized in Table 2. It was found that when bromothymol blue and phenolphthalein were added to the methanol solution of the sample, the colour changed significantly to blue and red, respectively. When 2,4-dinitroaniline indicator was added to the methanol solution of the sample, the colour changed only slightly. We believed that there were few basic sites with H- > 15.0 on the surface of the sample and it was difficult to determine the exact basic content. Therefore, in this paper we discuss the number of basic sites limited to two different surfaces, 9.8 > H- > 7.2 and H- > 9.8.

The activity of the KF/MgO catalyst was significantly higher than that of MgO alone. With increasing KF loading, the active sites were uniformly dispersed on the surface of MgO, so that the strong basicity and total alkalinity were increased, and a maximum basicity of 0.6 mmol/g was observed. However, the excessive KF content covered the active sites on the surface of the magnesia, resulting in a decrease in the alkalinity of KF. The influence of the calcination temperature on the catalytic performance was then studied. It is a very fascinating phenomenon that the uncalcined catalyst also has a high alkalinity, which probably catalyzes the transesterification reaction. It is well known that the furnace temperature is not sufficient to induce decarbonisation of the catalyst and its activity must be distributed to the fluoride anion. Therefore, as the calcination temperature increased from 80 ℃ to 300℃, the alkalinity of KF/MgO decreased. When the calcination temperature reached 500 ℃, the number and strength of the medium basicity of the active centre K_2MgF_4 reached the best, and the total alkalinity and medium basicity mainly led to the formation

Table 2 The alkali strength and amount of KF/MgO were tested by Hammett indicator meth

Catalyst	Basic strength (H–)	Basicity (mmol/g)		Total basicity (mmol/g)
		Weak	Medium	
		H– = 7.2–9.8	H– = 9.8–15	
MgO	H– < 7.2	–	–	–
5-KF/MgO-500	9.8 < H– < 15	0.04	0.018	0.058
30-KF/MgO-500	9.8 < H– < 15	0.21	0.05	0.26
40-KF/MgO-500	9.8 < H– < 15	0.38	0.22	0.6
45-KF/MgO-500	9.8 < H- < 15	0.42	0.16	0.58
40-KF/MgO-0	9.8 < H- < 15	0.34	0.12	0.46
40-KF/MgO-200	9.8 < H- < 15	0.15	0.11	0.26
40-KF/MgO-400	9.8 < H- < 15	0.23	0.19	0.42
40-KF/MgO-800	9.8 < H- < 15	0.42	0.14	0.56

of DC. The excessive calcination temperature caused the decomposition of the KF/MgO active components and the collapse of the catalyst pores, which caused the reaction rate to decrease.

Combined with the experimental results, the number and strength of the basic sites of the catalyst are closely related to the activity of the catalyst. The higher the number and strength of basic sites, the better the catalytic activity, which was more conducive to improving the reaction rate in the transesterification stage to obtain high yield DC.

Fourier transform infrared spectroscopy

The FT-IR characterization results for different KF/MgO catalysts are shown in Fig. 7. The result showed that 40-KF/MgO-200 had a strong absorption peak at 3600 cm^{-1}, which was attributed to the v(OH) stretching vibration in $Mg(OH)_2$ [35]. Combined with the above experimental results, the FT-IR patterns are in good agreement with the XRD results, and with the increase of calcination temperature, $Mg(OH)_2$ gradually transforms into MgO, and the absorption peak gradually decreases or even disappears, which was also similar to the Hammett analysis. The characteristic absorption peaks of CO_3 [2−] appeared at 1400 cm^{-1} and 1350 cm^{-1}, indicating that K_2CO_3 was formed when the catalyst was calcined in the muffle furnace.

Scanning electron microscopy

To further investigate the effects of different loadings and calcination temperatures on the morphology and structure of KF/MgO, we also carried out SEM analysis. As

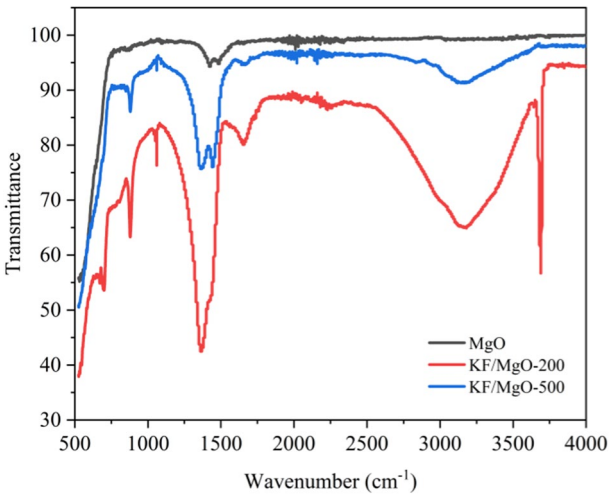

Fig. 7 FT-IR analysis and comparison of different KF/MgO catalysts

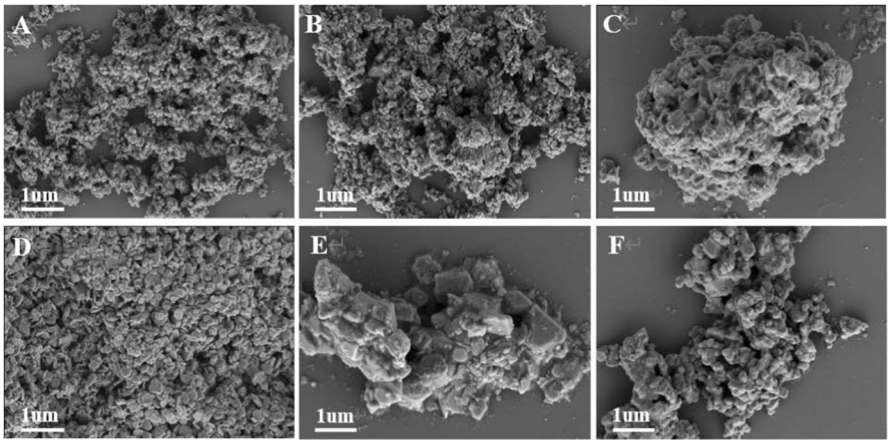

Fig. 8 SEM image of KF/MgO calcined at different KF loadings and temperatures. **a** 30-KF/MgO-500; **b** 40-KF/MgO-500; **c** 50-KF/MgO-500. **d** 40-KF/MgO-0; **e** 40-KF/MgO-200; **f** 40-KF/MgO-800

shown in Fig. 8, the change in particle size of KF/MgO at the same calcination temperature with increasing KF loading was not significant. Nevertheless, 50-KF/MgO-500 was overloaded with KF, causing the particle size and particles to combine and aggregate (C), which greatly reduced the catalytic performance or even inactivated KF/MgO. At a certain level of KF loading, the surface morphology of the KF/MgO catalyst before and after calcination is quite different. The 40-KF/MgO catalyst particles before calcination play a binding role due to the presence of crystalline water (D), which is manifested as a smooth structure with heterogeneous size and poor stability. However, the calcined 40-KF/MgO-800 catalyst has a severe collapse of its pore structure due to severe calcination (F), which is not conducive to the exposure of basic sites. Therefore, the appropriate loading and calcination temperature will make the KF/MgO catalyst undergo a good solid-phase reaction to form a new active

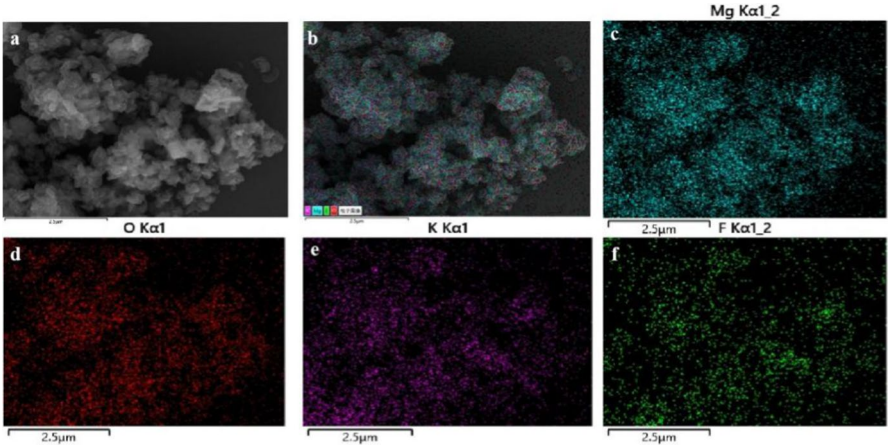

Fig. 9 SEM image of 40-KF/MgO-500 (**a**) EDS layered images (**b**) and Element mapping (**c**, **d**, **e**, **f**)

Table 3 Total distribution map spectrogram

Element	Wt %	Wt % sigma	At %
O	36.83	0.61	47.53
F	15.59	0.71	16.94
Mg	32.39	0.49	27.51
K	15.19	0.37	8.02
Amount	100.00		100.00

centre, so that the metal and support form mixture, prevent the catalyst from sintering, improve the activity and stability of the KF/MgO catalyst, and prolong its life.

In addition, SEM–EDS analyses were carried out on the 40-KF/MgO-500 material to reveal the distribution of Mg, O, K, and F elements on its surface. As shown in Fig. 9, Mg, O, K, and F elements are well dispersed on 40-KF/MgO-500 surface. Meanwhile, according to total distribution map spectrogram (Table 3), the atomic percentage of K element is half that of F element, indicating that the active centre of 40-KF/MgO-500 is K_2MgF_4, which has an excellent catalytic effect on ester exchange reactions. It can further prove that the 40-KF/MgO-500 had excellent catalytic activity.

Conclusion

In this paper, DC was synthesized via transesterification using DMC and IS as raw materials. Supported solid base catalysts were prepared to use the impregnation method, comprising KF/MgO that demonstrated high activity, stability, and easy separation. The influence of catalyst preparation and transesterification conditions on the synthesis of IS-PC prepolymer DC was researched. In conclusion, the temperature of calcination, catalyst loading, and dosage were identified as crucial factors that affect the catalyst's active centre, pore structure, and alkalinity. Under the given conditions of a transesterification temperature of 120 ℃, a raw material ratio of n(DMC)/n(IS) = 6.5, 40-KF/MgO-500 dosage of 0.21 wt %, and a 6 h transesterification reaction, the selectivity of DC was found to be the highest. It should be noted that an excessive use of the catalyst may result in an overly strong alkalinity, which can lead to side reactions during the transesterification phase. The study showed that at 500 ℃ calcination temperature and 40% KF loading, the in situ reaction of MgO under the stimulation of F^- produced new strongly basic active centres, namely K_2MgF_4 and K_2CO_3. In addition, the suitable pore structure increased the number of substrates on the catalyst surface, ultimately improving the catalytic performance.

Supplementary Information The online version contains supplementary material available at https://doi.org/10.1007/s11164-024-05279-5.

Acknowledgements Thanks are due to the financial support provided by the CAS project management, Party A, and the project lead (ZDRW-CN-2023-2-2). The contributions of all authors to the experimental work are also fully recognized

Author's contribution The manuscript was written through contributions of all authors. All authors have given approval to the final version of the manuscript.

Data availability All data have been included in the supplementary materials, and this manuscript does not report date generation or analysis.

Declarations

Conflict of interest There are no conflicts to declare.

References

1. Z.N. Diyana, R. Jumaidin, M.Z. Selamat, I. Ghazali, R.A. Llyas, Polymers **13**, 1396 (2021)
2. M.M. Tosif, A. Najda, A. Bains, G. Zawislak, G. Maj, P. Chawla, Polymers **13**, 2588 (2021)
3. D J Saxon, A M Luke H, Sajjad, W B Tolman, T M Reineke, *Prog Polym SCI*. 101 (2020)
4. M. Rose, R. Palkovits, Chemsuschem **5**, 167 (2012)
5. S. Chatti, G. Schwarz, H.R. Kricheldorf, Macromolecules **39**, 9064 (2006)
6. B.A.J. Noordover, D. Haveman, R. Duchateau, R.A.T.M.V. Benthem, C.E. Koing, JAPS. **121**, 1450 (2011)
7. A.M. Nelson, T.E. Long, POLYM INT. **61**, 1485 (2012)
8. M Yousfi, J Soulestin, S Marcille, M Lacrampe, *Polymer.* **217** (2021)
9. S Yum, H Kim, Y Seo, *Polymer*. **179** (2019)
10. Qian L, W Zhu , C Li, G Guan, D Zhang, Y Xiao, L Zheng, J. Polym. Sci. Pol CHDM. **51**, 1387 (2013)
11. W.J. Yoon, S.Y. Hwang, J.M. Koo, Y.J. Lee, S.U. Lee, S.S. Im, Macromolecules **46**, 7219 (2013)
12. S.M. Weidner, H.R. Kricheldorf, E Polym J. **49**, 2293 (2013)
13. J. Thiem, F. Bachmann, Makromol. Chem. **192**, 2163 (1991)
14. E.C. Varkey, K. Sreekumar, Mater. Sci. **45**, 1912 (2010)
15. C. Lee, H. Takagi, H. Okamoto, M. Kato, JAPS. **127**, 530–534 (2013)
16. F. Arico, P. Tundo, Beilstein J. Org. Chem. **12**, 2256–2266 (2016)
17. Y.S. Eo, H. Rhee, S. Shin, J. Ind. Eng. Chem. **37**, 42 (2016)
18. S.A. Park, J. Choi, S. Ju, J. Jegal, K.M. Lee, S.Y. Hwang, D.X. Oh, J. Park, Polymer **116**, 153 (2017)
19. Z. Yang, X. Li, F. Xu, W. Wang, Y. Shi, Z. Zhang, W. Fang, L. Liu, S. Zhang, Green Chem. **23**, 447 (2021)
20. W Fang , Y Zhang, Z Yang, Z Zhang, F Xu, W Wang, H He, Y Diao, Y Zhang and Y Luo, Appl Cata A Gen. **617** (2021)
21. Y. Ono, Appl. Catal. A gen. **155**, 133 (1997)
22. S. Fukuoka, I. Fukawa, T. Adachi, H. Fujita, N. Sugiyama, T. Sawa, Org. Process Res. Dev. **23**, 145 (2019)
23. O Gómez-de-Miranda-Jiménez-de-Aberasturi, A Centeno-Pedrazo, S P Fernández, R R Alonso, S Medel, J M Cuevas, L G Monsegue, S D Wildeman, E Benedetti, D Klein, H Henneken and J R, Green Chem. Lett. Rev. **14**, 534 (2021)
24. W. Qian, L. Liu, Z. Zhang, Q. Su, W. Zhao, W. Cheng, L. Dong, Z. Yang, R. Bai, F. Xu, Y. Zhang, S. Zhang, Green Chem. **22**, 2488 (2020)
25. L. Feng, W. Zhu, C. Li, G. Guan, D. Zhang, Y. Xiao, L. Zheng, Polymer Chem. **6**, 633 (2015)
26. C. Ma, F. Xu, W. Cheng, X. Tan, Q. Su, S. Zhang, ACS Sustainable Chem Eng. **6**, 2684 (2018)
27. M. Zhang, W. Lai, L. Su, G. Wu, Ind. Eng. Chem. Res. **57**, 4824 (2018)
28. W. Qian, X. Tan, Q. Su, W. Cheng, F. Xu, L. Dong, S. Zhang, Chemsuschem **12**, 1169 (2019)
29. O Gómez, J R, S Gil-Río, B Maestro-Madurga, O Gomez-Jimenez-Aberasturi, F Rıo-Perez, Arab. J. Chem. **12**, 4764 (2016)
30. M. Zhang, W. Lai, L. Su, G. Wu, Polym. Chem. **10**, 3380 (2019)
31. Z. Zhang, F. Xu, H. He, W. Ding, We Fang. W Sun, Z Li and S Zhang, Green Chem. **21**, 3891 (2019)
32. T. Wan, P. Yu, S. Gong, Q. Li, Y. Luo, Korean J. Chem. Eng. **25**, 998 (2008)

33. G. Fiorani, A. Perosa, M. Selva, RSC. **20**, 288 (2018)
34. Y. Wang, S.Y. Hu, Y.P. Guan, L.B. Wen, H.Y. Han, Catal. Lett. **131**, 574 (2009)
35. R. Kurosawa, M. Takeuchi, J. Ryu, JPCL. **10**, 5559 (2021)

Authors and Affiliations

Xiafeng Yang[1,2] · Xin Long[1] · Jianguo Li[1] · Qingyin Wang[1] · Gongying Wang[1,2] · Guangyuan Zhou[2,3]

✉ Gongying Wang
wanggongying1102@126.com

Xiafeng Yang
yangxiafeng20@mails.ucas.ac.cn

Xin Long
longx@cioc.ac.cn

Jianguo Li
ljguo369@126.com

Qingyin Wang
qingyinwang@cioc.ac.cn

Guangyuan Zhou
gyzhou@dicp.ac.cn

[1] Chengdu Institute of Organic Chemistry, National Engineering Research Center for Chiral Drugs and Materials, Chengdu 610041, Sichuan, China

[2] University of Chinese Academy of Sciences, Beijing 100049, China

[3] Dalian Institute of Chemical Physics, Chinese Academy of Sciences, Dalian 116023, Liaoning, China